

Structural, optical, and electrical characteristics of 70 MeV Si⁵⁺ ion irradiation-induced nanoclusters of gallium nitride

S. Suresh · V. Ganesh · U. P. Deshpande ·
T. Shripathi · K. Asokan · D. Kanjilal ·
K. Baskar

Received: 3 May 2010 / Accepted: 23 August 2010 / Published online: 8 September 2010
© Springer Science+Business Media, LLC 2010

Abstract We report the formation of nanoclusters on the surface of gallium nitride (GaN) epilayers due to irradiation with 70 MeV Si ions with the fluences of 1×10^{12} ions/cm² at the liquid nitrogen temperature (77 K). GaN epilayers were grown using a metal organic chemical vapor deposition system. Omega scan rocking curves of (002) and (101) plane reflection shows irradiation-induced broadening. Atomic force microscopy imagery revealed the formation of nanoclusters on the surface of the irradiated samples. X-ray photoelectron spectroscopy confirms that the surface features are composed of GaN. The effects of ion-beam-produced lattice defects on the surface, electrical, and optical properties of GaN were studied and possible mechanisms responsible for the formation of nanoclusters during irradiation have been discussed.

Introduction

Gallium nitride (GaN) is one of the most important semiconductor materials with superior radiation hardness compared with other compound semiconductors like GaAs and InP due to the strong bond strength and wide bandgap [1–3]. Swift heavy ions (SHI) of tens of MeVs have been

established as an excellent tool for nano-structuring of thin films and surfaces. Such heavy ion deposits a huge amount of kinetic energy almost instantaneously into a highly localized volume of nanodimensions. Energy dissipation in to the relatively cold surrounding occurs approximately, within few tens of picoseconds and leads to rapid solidification of the excited volume. This highly localized process can be regarded as a transient melting and rapid quenching mechanism, which drives the solid far from equilibrium and often modifies the surface with structures of non-equilibrium material in nanodimensions. Recent studies suggest that SHI impacts can be used to generate spatially separated nano-scale structures with the application of high-ion fluences, this process can result in structural instabilities and a corresponding, often periodic, nano-scale patterning of surfaces and thin films [4]. The ultra-fast solid–liquid–solid phase transition in the surrounding material, and the direct modification of the material in the track itself can create new potential gradients, which may then act as a driving force for further modification during the ongoing ion irradiation. When increasing the ion fluence, and thus, the number of modified zones, the interaction, and finally, the overlap of these zones may give rise to surface instabilities and self-organization effects. Such processes often result in large area coverage and sometimes periodic nanometric patterns and structures [5].

In recent studies, the impact of ion irradiations on the structural, optical, and electrical properties of GaN has been explored. GaN layers grown by metal organic chemical vapor deposition (MOCVD) were irradiated with 100 MeV silver and oxygen ions, 70 MeV nitrogen ions, 75 MeV tin ions [6–8], and 80 MeV Si ions [9] to study the changes in the crystal quality due to irradiation at room temperature. In the present investigation, results of experiment aimed to form nano-structures on the surface of GaN

S. Suresh (✉) · V. Ganesh · K. Baskar
Crystal Growth Centre, Anna University, Chennai 600 025, India
e-mail: suresh9111@gmail.com

U. P. Deshpande · T. Shripathi
UGC-DAE Consortium for Scientific Research, University
Campus, Khandwa Road, Indore 452001, Madhya Pradesh, India

K. Asokan · D. Kanjilal
Inter University Accelerator Centre, Aruna Asaf Ali Marg,
New Delhi 110067, India

by ion irradiation are reported. Surface modifications induced by 70 MeV Si^{5+} ion irradiation at liquid nitrogen temperature on MOCVD grown GaN has been studied with atomic force microscopy (AFM) and X-ray photoelectron spectroscopy (XPS). The ions effects on the structural, optical, and electrical properties were also studied and a suitable mechanism responsible for the observed changes of those properties is proposed.

Experiment

About 3 μm thick GaN epilayers were grown on sapphire substrates using the MOCVD technique. The samples were grown at 1,075 $^{\circ}\text{C}$ after depositing a 30 nm thick GaN at low temperature as a buffer layer using trimethylgallium and ammonia as precursors. The samples were irradiated with 70 MeV Si^{5+} ions with a fluence of 1×10^{10} , 1×10^{11} and 1×10^{12} ions/ cm^2 using the 15 UD tandem pelletron accelerator [10]. The irradiation experiments were carried out at liquid nitrogen temperature (77 K). According to the calculations of stopping ranges of ions in matter (SRIM) [11], the projected range of 70 MeV Si^{5+} ions in GaN was found to be $\sim 12.68 \mu\text{m}$. This shows that the Si ions pass through the 3 μm thick GaN matrix. Structural properties were studied before and after irradiation using Cu-K α X-ray from Philips Xpert X-ray diffractometer. The irradiation-induced surface modifications were studied using Nanoscope IIIA AFM. The chemical nature of the surface was studied using XPS.

Results and discussion

Stopping ranges of ions in matter calculations

In order to understand the modifications induced by ion irradiation in GaN, it is important to analyze the role of associated energy loss mechanisms. It is well known that when an energetic ion penetrates into any material, it loses energy by two nearly independent processes: elastic collisions with the nuclei, known as nuclear energy loss S_n , and inelastic collisions of the highly charged projectile ion with atomic electrons of the matter, known as electronic energy loss S_e . In the inelastic collision, the energy is transferred from the projectile to the atoms through excitation and ionization of the surrounding electrons. The nuclear energy loss of 70 MeV Si^{5+} ions is three orders of magnitude smaller than the electronic energy loss in GaN target material as shown in Fig. 1. Therefore, the maximum energy deposited to the material is expected to be mainly due to the electronic energy loss during the passage of ions through the GaN matrix. The layer suffers uniform

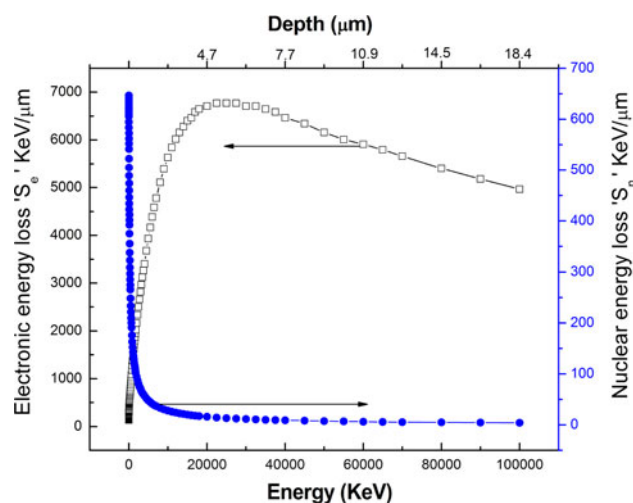


Fig. 1 SRIM calculation showing the variation of nuclear and electronic energy loss with ion energy and projectile depth

irradiation effects as the projected ion range is greater than the thickness of the layer. The damage caused due to the linear energy transfer ($S_n + S_e$) is 9.289 MeV/(mg/ cm^2) in GaN target, S_n and S_e were obtained using SRIM program simulating the irradiation conditions [11].

High-resolution X-ray diffraction

High-resolution X-ray diffraction rocking curves of the samples were recorded for the reflection planes of (002) and (101). ω - 2θ scan rocking curves of (101) asymmetric reflection plane of pristine and irradiated GaN samples are shown in Fig. 2. The absence of a shift in the peak values implies that there is no irradiation-induced phase change or strain in the crystalline material. These results are consistent with previous studies carried out with high energy Au^{7+} and Sn^{5+} ion irradiation experiments wherein it was shown that degradation in the crystallinity of GaN occurs at the fluence of 5×10^{13} ions/ cm^2 [12, 13]. The fluence used in this study is very low compared to those used in the previous study, and hence, the possibility of amorphisation can be ruled out. Full width at half maximum (FWHM) of the (101) asymmetric plane ω - 2θ rocking curve scans, which directly measure the crystalline quality of the epilayers, is shown in Fig. 3 with respect to ion fluence. As the ion fluences increases, the FWHM also increases from 529 to 651 arc-sec. FWHM of (002) reflection plane also showed a marginal increase with respect to ion fluence, it increases from 240 to 260 arc-sec. This indicates that there is no localized amorphisation at 1×10^{10} ions/ cm^2 ion fluence whereas the irradiation-induced damages increases with increasing ion fluence causing the broadening of the rocking curves.

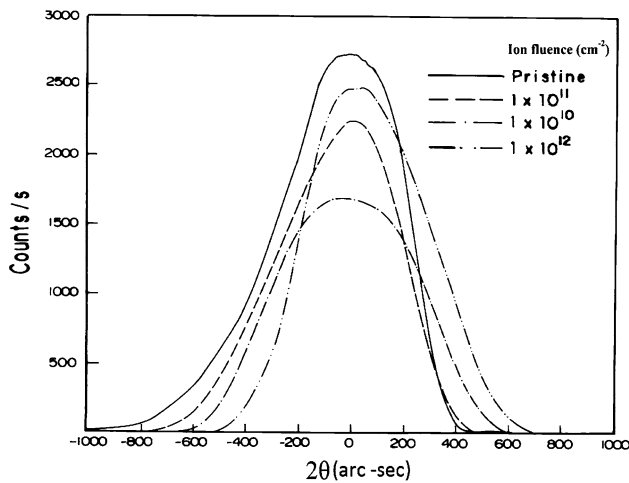


Fig. 2 The ω - 2θ rocking curves for pristine and 70 MeV Si^{5+} ion irradiated GaN films measured for (101) Bragg plane

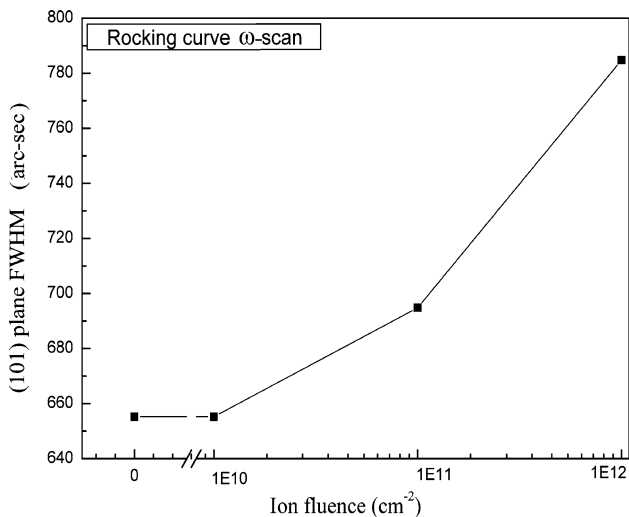


Fig. 3 The ω - 2θ rocking curves FWHM of (101) plane for pristine and 70 MeV Si^{5+} ion irradiated GaN films

Atomic force microscopy

Figure 4 shows $2 \times 2 \mu\text{m}^2$ 3D AFM scans of the pristine and the irradiated samples. Pristine GaN layer has wide surface steps and terraces which are the normal features of high-quality GaN [14]. After irradiation, the sample surface steps and terraces disappeared and the clusters of nano dimensions were formed as shown in Fig. 4b. It is clear from the Fig. 4c, d that the cluster size on the surface of the irradiated sample increases with an increase in ion fluence. The RMS roughness for the pristine and irradiated samples is 0.5 nm, 0.5 nm (1×10^{10}), 0.7 nm (1×10^{11}), 1.1 nm (1×10^{12}), respectively, as shown in Fig. 5. It is interesting to note that the surface roughness for the samples irradiated with the fluence of 1×10^{10} ions/cm² has not been altered, which may be attributed to the nanocluster formation,

which eliminates the surface steps and compensates the surface roughness.

Nanocluster formation mechanism

The changes in surface morphology were created due to electronic energy transfer and the deposition of large kinetic energy by the irradiated ions instantaneously on the GaN surface [15]. For large electronic energy loss of the ion, a cylindrical zone of the order of ~ 5 nm in diameter will form along the ions path [16], with high atomic mobility and reduced density. Depending on the material and irradiation conditions, the irradiated region may be strikingly different from the pristine [17]. The effects of the high temperature and high pressure on the surrounding material and also the direct modification of the material in the track itself can create new potential gradients, which then act as a driving force for further modification and create nano-structures during ion irradiations.

X-ray photoelectron spectroscopy

Figure 6 shows full scan XPS spectra from (a) Si ion irradiated GaN sample (ion fluence 1×10^{12} ions/cm²) and (b) pristine GaN sample. Ga, N, C, and O peaks are visible in all the spectra. The C and O background peaks originate from organic compound precursors used during MOCVD. No shift and tails were observed in the XPS peaks as shown in the inset of Fig. 6, hence, the nanoclusters formed on the surface may not be Metal Ga droplets, which would otherwise have resulted in a shift of the Ga peaks toward lower energies [18]. In the present investigation, the change in the carbon concentration of pristine irradiated and surface-cleaned irradiated GaN (cleaned by Ar ion sputtering) were negligible confirming that there is no additional carbon deposition during irradiation, and the present carbon impurity was deposited during GaN growth by MOCVD. Hence, we may conclude that the nanoclusters seen in the AFM images are composed of GaN.

Hall effect measurements

The carrier concentration and hall mobility for the unirradiated and irradiated samples are shown in Fig. 7. The measurements indicate that new donors were introduced by the irradiation up to certain fluence of 1×10^{11} ions/cm². This suggests that the irradiation mainly creates N Frenkel pairs, V_N-N_I , in which V_N is a donor, as expected, and N_I is an acceptor, as predicted by theory [19, 20]. The reduction in carrier density at fluence of 1×10^{12} ions/cm² is a net result of trapping by radiation-induced trap levels and charge compensation by created defects with opposite character [21]. The Hall mobility as shown in the Fig. 7

Fig. 4 AFM images **a** as grown, **b** irradiated with 1×10^{10} ions/cm² fluence, **c** irradiated with 1×10^{11} ions/cm² fluence, **d** irradiated with 1×10^{12} ions/cm² fluence

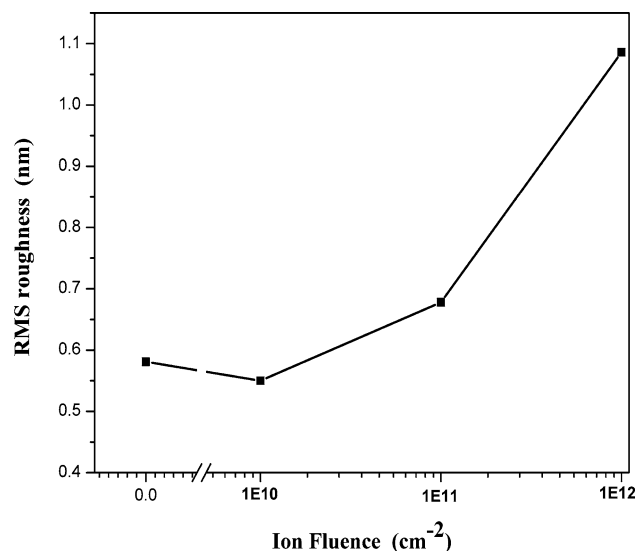
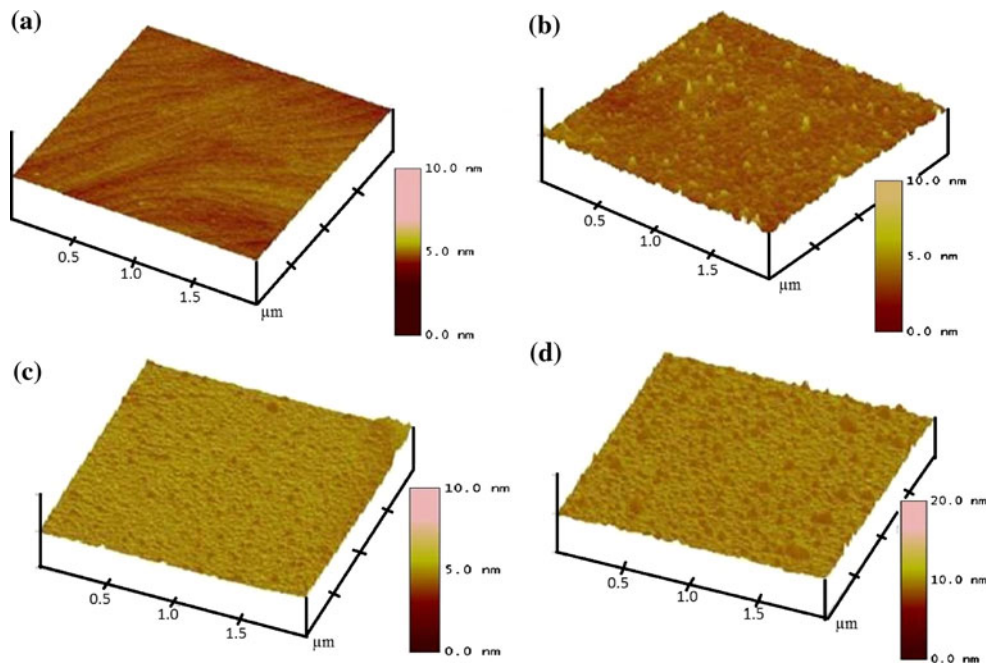


Fig. 5 RMS roughness of pristine and the irradiated GaN epilayers as a function of ion fluence

decreases due to coulombic scattering caused by an increasing number of traps in GaN from radiation induced defects, that results in increased concentration of charged scattering centers, and hence decreased electron mobility [22].

Photoluminescence studies

Figure 8a shows the normalized photoluminescence (PL) spectra for the pristine and irradiated samples. Near bandedge emission (NBE) occurs at 3.429 eV for pristine GaN epilayer. The NBE red shifts from 3.429 to 3.422 eV

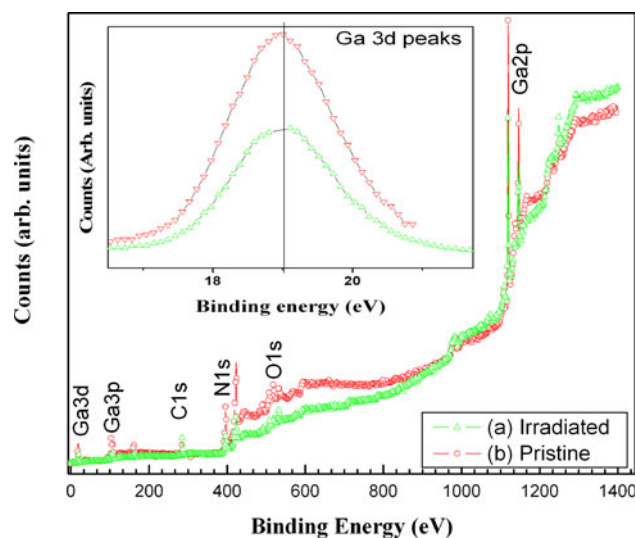


Fig. 6 Full scan X-ray photoelectron spectrum of **a** irradiated GaN and **b** pristine GaN. *Inset* shows detailed scans of the Ga3d peak for irradiated GaN and pristine GaN

and broadens on increasing the ion fluence indicating the presence of tensile stress. This may be attributed to the formation of nanoclusters as evident in the AFM images shown in Fig. 4a–d and subsequent defect production induced by ion irradiation. Generation of defects due to ion irradiation increases on increasing the ion fluences from 1×10^{10} to 1×10^{12} ions/cm² resulting in an increase in tensile stress causing a further red shift in NBE and subsequently reducing the luminescence intensity in the irradiated samples. These effects may also be due to the efficient self-absorption effects.

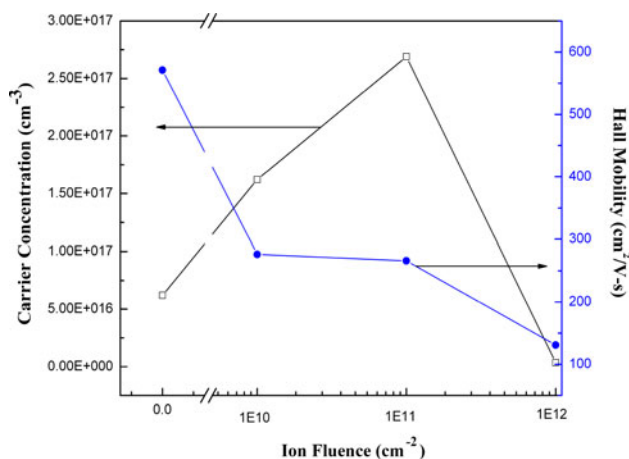


Fig. 7 Variation of carrier concentration and hall mobility of the pristine and irradiated samples with respect to irradiation fluence

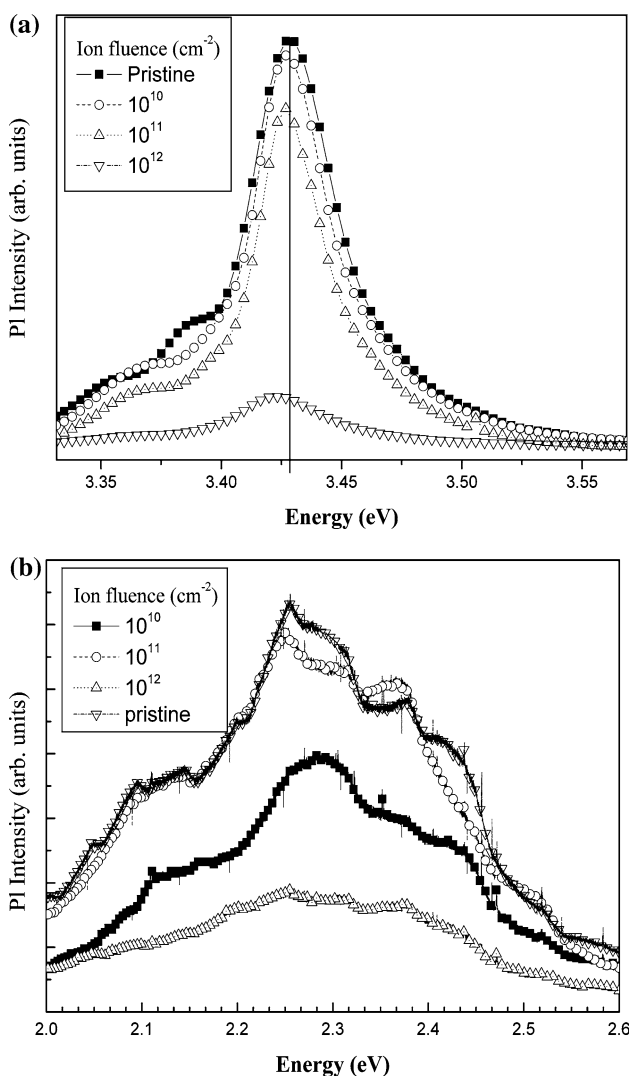


Fig. 8 **a** Photoluminescence spectra recorded at room temperature showing the near band emission of the pristine and the irradiated samples. **b** Yellow luminescence of the pristine and the irradiated samples

Broad yellow luminescence was observed from 2.0 to 2.6 eV with maximum at 2.25 eV as shown in Fig. 8b. This emission may be due to the deep levels at the bandgap of the material created by the defects and impurities complexes [19, 23]. It is interesting to note a decrease in the YL band intensity at the fluence of 1×10^{10} ions/cm² compared with the pristine sample. This may be due to the combined effect of the creation of photoelectron recombination channels due to the introduction of irradiation-induced defects and a decrease in defects responsible for YL which might have been annealed out during restructuring of the lattice while forming nanoclusters. For fluence of 1×10^{11} ions/cm² the YL intensity reached the same level as that of pristine samples due to increase in the concentration of defects causing YL. In Fig. 9, relative intensity, the ratio between near band edge emission intensity I_b and defect intensity I_d , was plotted as a function of ion fluence. It clearly shows that at 1×10^{10} ions/cm² fluence, YL is low with respect to near band emission, and relative intensity decreases almost thrice at 1×10^{12} ions/cm² fluences. This may be attributed to the generation of defects which may act as trapping centers affecting the luminescence properties of the material.

UV–visible spectroscopy

The absorption coefficient as a function of energy has been plotted in Fig. 10 to find the variation of band gap due to irradiation. The absorption band edge of the pristine GaN is at 3.4 eV as shown in the inset of Fig. 10. High-energy irradiation usually induces band tailing effects which seriously affect the optical properties of the material [10, 12]. A red shift in the absorption band edge with a decrease in

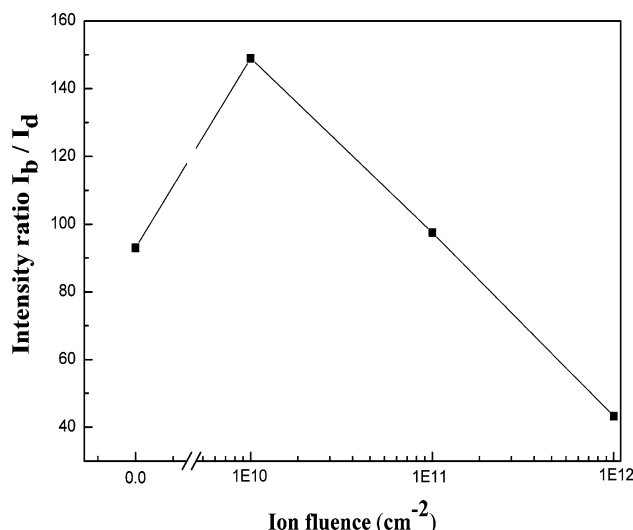


Fig. 9 Relative intensity of the near band emission intensity I_b to the defect emission intensity I_d as a function of ion fluence

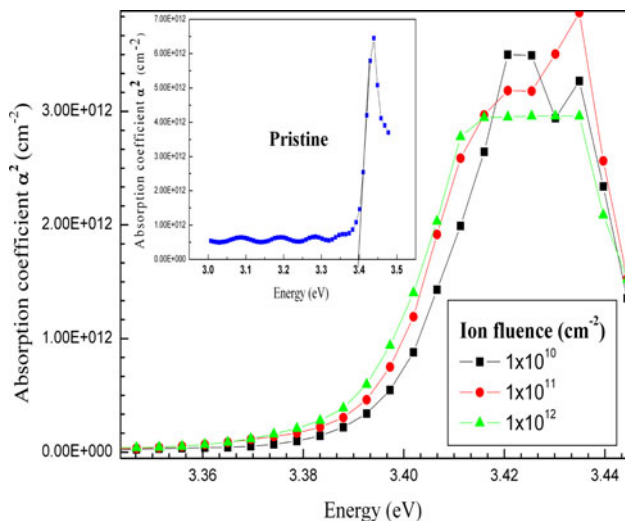


Fig. 10 Plot of α^2 versus energy for the epitaxial layers irradiated with different ion fluences. *Inset* of the figure showing the band edge at 3.4 eV for the unirradiated sample

the slope is observed with ion fluence. This indicates that the absorption band edge become less steep after irradiation due to the band tailing effect as supported by the broadening and a red shift in the PL NBE. Such change in absorption band edge may be due to the tensile stress generated strain near the defects created by the Si^{5+} ion irradiation [24].

Conclusion

X-ray diffraction studies showed no irradiation-induced structural phase transformation in the epilayer, with only an increase in FWHM due to surface modifications and irradiation damage. The formation of GaN nanoclusters on the surface of GaN epilayers grown by MOCVD was confirmed with AFM images and XPS studies. The irradiated samples were characterized to study the modification in electrical and optical properties. These results show that by suitably adjusting the irradiation conditions and inducing further driving forces, morphologically well-aligned nanostructures can be obtained by SHI irradiation on GaN thin films without much alteration in their characteristics.

Acknowledgements The authors wish to thank the Department of Science and Technology (DST), India, for the financial support, Dr. B.K. Panigrahi, Indira Gandhi Centre for Atomic Research, Kalpakkam, and UGC-DAE CSR, Indore for extending the characterization facility.

References

1. Pearton SJ, Zolper JC, Shul RJ, Ren F (1999) *J Appl Phys* 86:1
2. Kucheyev SO, Williams JS, Pearton SJ (2001) *Mater Sci Eng R* 3:108
3. Amano H, Akasaki I, Kozawa T, Hiramatsu K, Sawaki N, Ikeda K, Ishii Y (1988) *J Lumin* 40:121
4. Bolse W, Schattat B, Feyh A (2003) *Appl Phys A* 77:11
5. Bolse W (2006) *Nucl Instrum Methods Phys Res B* 244:8
6. Herre O, Wesch W, Wendler E, Gaiduk PI, Komarov FF, Klaumunzer S, Meier P (1998) *Phys Rev B* 58:4832
7. Premchander P, Abhaya S, Sivaji K, Amarendra G, Baskar K, Lee YT (2006) *Physica B* 376:507
8. Suresh Kumar V, Puviarasu P, Thangaraju K, Thangavel R, Baranwal V, Singh F, Mohanty T, Kanjilal D, Asokan K, Kumar J (2006) *Nucl Instrum Methods Phys Res B* 244:145
9. Varadarajan E, Dhanasekaran R, Avasthi DK, Kumar J (2006) *Mater Sci Eng B* 129:121
10. Kanjilal D (2001) *Curr Sci* 80:560
11. Ziegler JF, Biersack JP, Littmark U (eds) (1985) *The stopping and ranges of ions in solids*. Pergamon, New York. <http://www.srim.org>
12. Premchander P, Sonia G, Baskar K (2004) *Jpn J Appl Phys* 43:4150
13. Suresh Kumar V, Senthil Kumar M, Puviarasu P, Kumar J, Mohanty T, Kanjilal D, Asokan K, Tripathi A, Fontana M, Camarani A (2007) *Semicond Sci Technol* 22:511
14. Heying B, Tarsa EJ, Elsass CR, Fini P, DenBaars SP, Speck JS (1999) *J Appl Phys* 85:6470
15. Kucheyev SO, Timmers H, Zou J, Williams JS, Jagadish C, Li G (2004) *J Appl Phys* 95:3048
16. Mohanty T, Satyam PV, Mishra NC, Kanjilal D (2003) *Radiat Meas* 36:137
17. Gossick BR (1959) *J Appl Phys* 30:1214
18. Choi HW, Rana MA, Chual SJ, Osipowicz T, Pan JS (2002) *Semicond Sci Technol* 17:1125
19. Neugebauer J, Van de Walle CG (1996) *Appl Phys Lett* 69:503
20. Boguslawski P, Briggs EL, Bernholc J (1995) *Phys Rev B* 51:17255
21. Look DC, Sizelove JR (1987) *J Appl Phys* 62:3660
22. Look DC (1997) *Mater Sci Eng B* 50:50
23. Reshchikov MA, Morkoc H (2005) *J Appl Phys* 97:061301
24. Burkig VC, McNichols JL, Ginell WS (1969) *J Appl Phys* 40:3268